Journal of Applied Polymer Science

Tailoring in thermomechanical properties of ethylene propylene diene monomer elastomer with silane functionalized multiwalled carbon nanotubes

Sadia Sagar Iqbal,[1] Nadeem Iqbal,[2] Tahir Jamil,[1] Arshad Bashir,[3] Zaffer M. Khan[4]

[1]Department of Polymer Engineering and Technology, CEET, University of the Punjab, Lahore, Pakistan
[2]Centre for Undergraduate Studies, University of the Punjab, Lahore, Pakistan
[3]School of Chemical and Materials Engineering, National University of Sciences and Technology, Islamabad, Pakistan
[4]Institute of Space Technology, Islamabad, Pakistan
Correspondence to: S. S. Iqbal (E-mail: sadiasagariqbal.pu@gmail.com)

ABSTRACT: The incorporation of silane treated multiwalled carbon nanotubes (S-MWCNTs) is used as an effective path for tailoring thermomechanical properties of ethylene propylene diene monomer (EPDM). In this study, S-MWCNTs were introduced into EPDM using internal dispersion kneader and two roller mixing mill. By altering the mass ratio of S-MWCNTs from 0 to 1, thermal conductivity, thermal stability and phase transition temperatures and their respective enthalpies are discussed of the fabricated nanocomposites. It is observed that silane modification improves their dispersion and increases the interfacial bonding between MWCNTs and polymer matrix. Scanning electron microscopy along energy dispersive spectroscopy analysis is performed to confirm the silane functionalized MWCNTs are selectively distributed in the host polymer. More importantly, an important increase in mechanical properties like ultimate tensile strength and hardness is achieved through introducing silane functionalized MWCNTs. © 2015 Wiley Periodicals, Inc. J. Appl. Polym. Sci. **2016**, *133*, 43221.

KEYWORDS: composites; differential scanning calorimetry; graphene and fullerenes; mechanical properties; nanotubes

Received 4 August 2015; accepted 13 November 2015
DOI: 10.1002/app.43221

INTRODUCTION

Inorganic/organic nanofillers (nanorods, nanotubes and nanofibers) have been used to fabricate nanocomposites for specific applications. These nanoscale reinforcements enhance thermal, electrical, magnetic, and mechanical properties of the host matrices due to their large specific surface area and nanoscale interaction with the recipient.[1] Adohi *et al.*[2] reported that CNTs provide fine tuning of electronic, magnetic, and structural properties of polymer matrix. Polymer nanocomposites (PNCs) are being used in a variety of fields, such as aerospace, automobile, medical, and construction. PNCs usually have low density with high strength to weight ratio as compared to metal and ceramic matrix composites. Multiwalled carbon nanotubes (MWCNTs) are used as reinforcing filler in PNCs due to its outstanding strength, thermal stability, electromagnetic effects, and fire retardant capability.[3–5] The first polymer nanocomposites using carbon nanotubes as filler were reported in 1994 by Ajayan *et al.*[6] To employ MWCNTs as effective reinforcement in polymer nanocomposites, proper dispersion and appropriate interfacial adhesion between the MWCNTs and polymer matrix have to be guaranteed. Many research efforts have been directed towards producing nanoreinforcement/polymer composites for functional and structural applications.[7–9] However, even after a decade of research, the full potential of employing nanoreinforcements has been severely limited because of the difficulties associated with dispersion during processing and poor interfacial interaction between nanofiller and polymer matrix. The reviews by Sung *et al.*[10] and Dyke *et al.*[11] give an overview of the current state of the open-end and sidewall covalent functionalization of nanotubes, respectively. The nature of dispersion problem for nanofiller is rather different from other conventional (microsize) fillers, such as spherical particles and carbon fibers. It happened because nanofiller like MWCNTs having small diameter and high aspect ratio are characterized by extremely large surface area.[12] In addition, the physical nature and chemical structure of particles also play an important role in uniform dispersion of nanofiller into polymer matrix. In order to enhance filler/fiber to polymer interaction/compatibility, the reinforcements have to be functionalized/

modified. There is much method which is used to functionalize MWCNTs like Acid treatment, base treatment, amine functionalization, organic functionalization (phenol functionalization), etc.

EPDM is a type of saturated synthetic elastomeric polymer. Its performance in light, oxygen, heat, and particularly ozone atmosphere is significant. The key parameters of EPDM are relative contents of ethylene in the polymer chains and the alternation in the comonomer composition of diverse chains. EPM and EPDM elastomers with ethylene contents greater than 60 mol % are increasingly crystalline and are tough. EPM can be vulcanized radically using peroxide crosslinkers. The existence of third diene monomer in EPDM approves conventional sulphur vulcanization and other vulcanization systems like resins at the pendant sites of unsaturation. Various fillers like carbon black, silica, clays, etc are introduced into the EPDM polymer to acquire the desired mechanical, thermal, and electrical properties.[13–17]

In the present novel study, silane modified multiwalled carbon nanotubes with multiple concentrations were introduced into the ethylene propylene diene monomer elastomeric matrix using internal dispersion kneader/two roller mixing mill to investigate the effects of S-MWCNTs on their thermal conductivity, and thermal degradation/heat absorbing capability. Isothermal behavior (phase transition temperature and their respective enthalpies) was calculated to access the use of fabricated nanocomposite for right environment. In addition, tensile strength, elongation at break, charred surface analysis, and elastomeric hardness were also examined to determine the potential applications of the nanocomposites for thermal protection systems.

EXPERIMENTAL

Materials

3-Aminopropyl-trimethoxysilane (APTMS) and cetrimonium bromide (CTAB) were purchased from Sigma-Aldrich, Germany. Carbon black, sulphur, zinc oxide, and stearic acid were acquired from Merck. MBTS (Mercapto benzothiazoles) and cyclohexyl benzthiazyl sulphenamide (HBS) were procured from Dalian Richon Chemical. Aromatic oil and wax were bought from International petrochemicals. EPDM elastomer (KELTAN 4331A) used as a matrix in the present investigation was supplied by Technical Rubber Products. The armchair ($m \neq n$) MWCNTs was used to fabricate the composite specimen. MWCNTs are fabricated through CVD method using Fe as catalyst. They have purity >95%, diameter 20–30 nm, length 50–70 μm, and average aspect ratio 2400:1). MWCNTs were purchased from Nanoport, and were used as received.

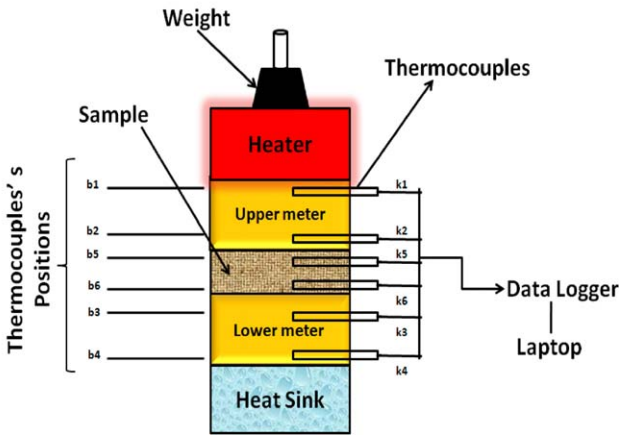

Figure 1. Experimental setup for the measurement of thermal conductivity of the fabricated elastomeric nanocomposites. [Color figure can be viewed in the online issue, which is available at wileyonlinelibrary.com.]

Characterization

To appraise thermal conductivity (TC) of the fabricated polymer nanocomposites, the apparatus were designed and developed domestically. The ASTM E1225-99 was used to evaluate thermal conductivity of the rubber nanocomposites. The graphical representation of the comparative guarded longitudinal heat flow system is demonstrated in Figure 1 which shows the possible locations of temperature sensors, heating source, water heat sinker, lower/upper meter bars, testing sample, temperature data logger, and a laptop. Lower and upper meter bar are made of 99.9% pure copper material. Time–temperature contours of all thermocouples located at specific positions were displayed on the laptop screen through "Squirrel OQ610 series" temperature data logger. Thermal conductivity of the composite specimens was measured using eq. (1).

$$\text{Thermal conductivity of specimen} = \text{TC} = ((X'_{\text{T}} + X'_{\text{B}})(b_4 - b_3))/2(k_4 - k_3) \quad (1)$$

where

Heat flow at top

$$\text{bar} = X'_{\text{T}} = \lambda_{\text{m}}(k_2 - k_1)/(b_2 - b_1)$$

Heat flow at bottom

$$\text{bar} = X'_{\text{B}} = \lambda_{\text{m}}(k_6 - k_5)/(b_6 - b_5)$$

λ_{m} = Thermal conductivity of the copper meter bar

k_1, k_2, k_3, k_4, k_5, and k_6 are the temperatures of six thermocouples and b_1, b_2, b_3, b_4, b_5, and b_6 are the corresponding positions of these six thermocouples.

Table I. Basic Formulation of EPDM Composite

EPDM (wt %)	Carbon black (wt %)	ZnO (wt %)	Stearic acid (wt %)	Aromatic oil (wt %)	Sulphur (wt %)	MBTS (wt %)[a]	HBS (wt %)[b]
100	20	5	2	7.5	2	2.5	2

[a] MBTS: Mercaptobenzthiazole disulphide.
[b] Cyclohexyl benzthiazyl sulphenamide (HBS).

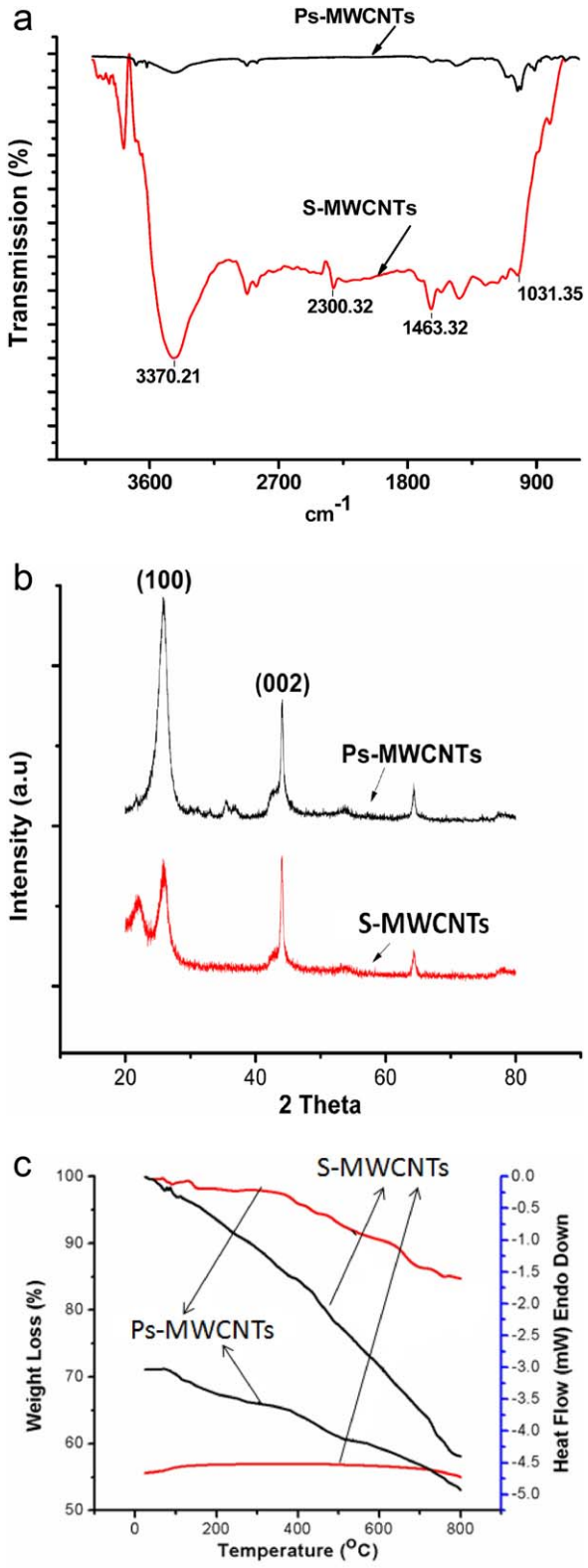

Figure 2. (a) FTIR spectra for Ps-MWCNTs and S-MWCNTs. (b) XDR pattern for Ps-MWCNTs and S-MWCNTs. (c) TG/DTA thermographs of Ps/S-MWCNTs. [Color figure can be viewed in the online issue, which is available at wileyonlinelibrary.com.]

Thermal stability and heat flow response of the polymer composites were characterized using Perkin Elmer Diamond TG/DTA. Heating rate and temperature range during the Thermogravimetric and differential thermal analyses of the specimens was 10°C min^{-1} and 25–800°C, respectively. Perkin Elmer Diamond DSC was used to analyzed physical transformations viz. phase transitions (glass, crystallization, and melting) and specific enthalpies of the fabricated samples with heating rate 10°C min^{-1} from 75 to 450°C.

Tensile strength, elongation at break, and modulus of elasticity of the polymer nanocomposites were executed using universal tensile testing machine (AG-20KNXD Plus, Shimadzu) according to the ASTM D412-98A. Shore A rubber hardness of the composite specimens were carried out using Torsee testing machine.

Scanning electron microscopy (SEM, JSM 6940A, Jeol) along with the energy dispersive spectroscopy was used to analyze the surface morphology of the post-thermal conductivity tested specimens and compositional analysis of the rubber nanocomposite.

Fourier transformation infrared (FT-IR) spectroscopy in which infrared spectrum measures the quantity of radiation absorbed as a function of its frequency. Four samples of KBr with 0.5% by mass of MWCNTs were prepared for FT-IR spectrometer. To obtain these samples, MWCNTs were mechanically mixed to the KBr powder and pressed into discs shape. FT-IR (Perkin-Elmer Diamond 1000) was used to analyze the changes taken place on the S-MWCNTs surface due to the silane treatment in the frequency range 400–4000 cm^{-1}.

The degree of crystallinity of the pristine/silane functionalized MWCNTs was characterized by powder X-ray diffraction (XRD). XRD measurements were recorded using an X-ray diffractometer (STOE) equipped with a back monochromator operating at 40 kV and 40 mA, and a copper cathode was used as X-ray source ($\lambda = 0.154$ nm and $a = 1.54060$ Å). XRD patterns were recorded from 10° to 80° (2θ) with a scanning step of 0.02 s^{-1}.

Surface Modification of MWCNTs

A silane coupling agent [3-aminopropyl-trimethoxysilane (APTMS)] along with CTAB was used for the surface modification of the MWCNTs. To modify the surface of pristine multiwalled carbon nanotubes (Ps-MWCNTs), first purification was performed at 400°C with heating rate *viz.* 10°C/min for 12 h followed by their treatment with hydrochloric acid to remove impurities *viz.* metal traces, amorphous carbon and other impurities from heat treated MWCNTs. In the second step, purified MWCNTs were immersed in toluene at room temperature. Then, MWCNT/toluene solution was sonicated in ultrasonicator bath at 40 kHz, 90°C for 40 min. After that, 1 wt % CTAB was added in the preset mixture followed by further sonication at 70° with 40 kHz for next 50 min to deagglomerate the MWCNTs. Subsequently, 5 vol % SCA was added in the mixture and sonicated at 40 kHz for next 4 h at 90°C to attain silane moieties. Next, magnetic stirring followed at 1000 rpm for 2 h at 120°C was experienced. The sonicated solution was then diluted five times and washed six times to maintain its pH level

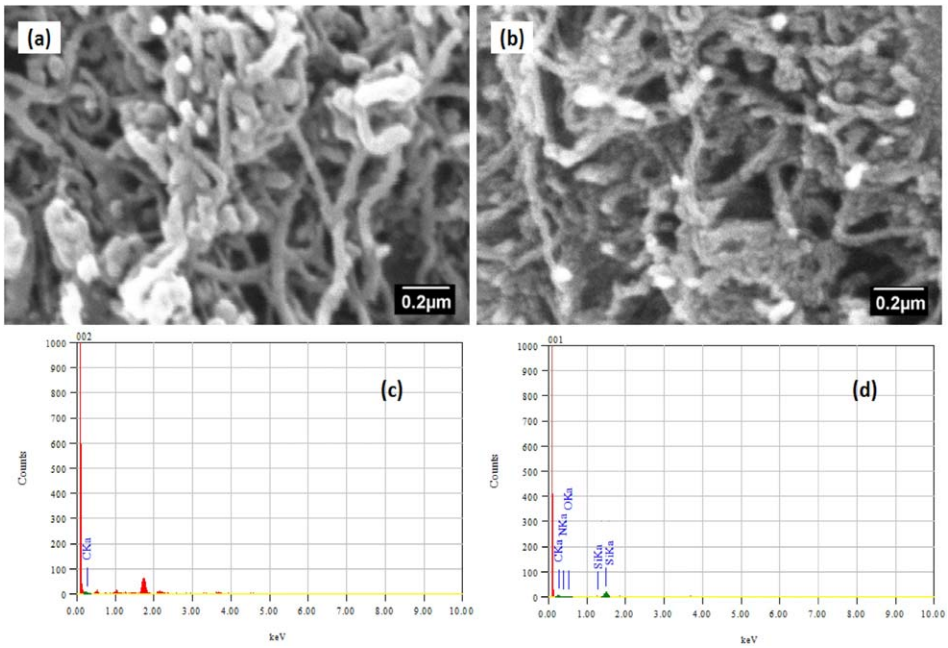

Figure 3. SEM micrographs along EDS analysis of Ps-MWCNTs (a) and S-MWCNTs (b). [Color figure can be viewed in the online issue, which is available at wileyonlinelibrary.com.]

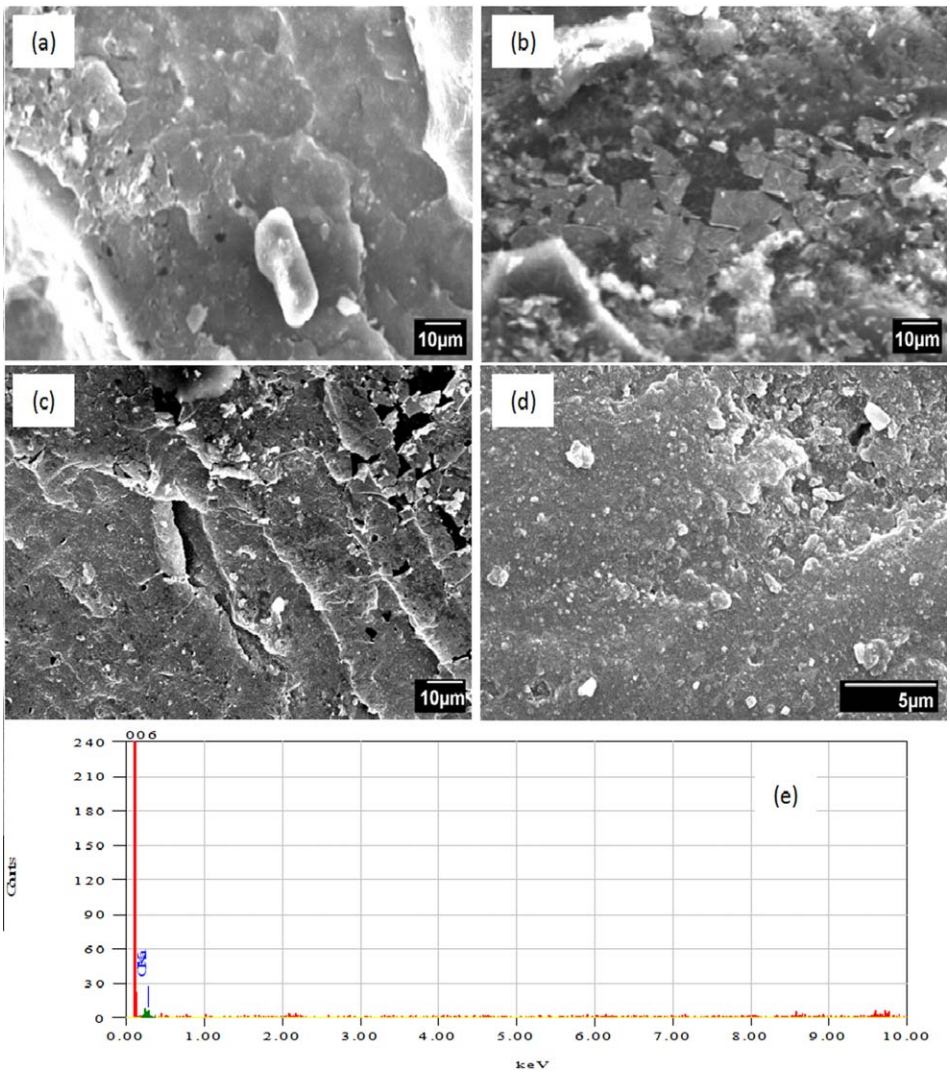

Figure 4. Distribution of P-MWCNTs within the polymer matrix (a–d), compositional analysis of the embedded P-MWCNTs (e). [Color figure can be viewed in the online issue, which is available at wileyonlinelibrary.com.]

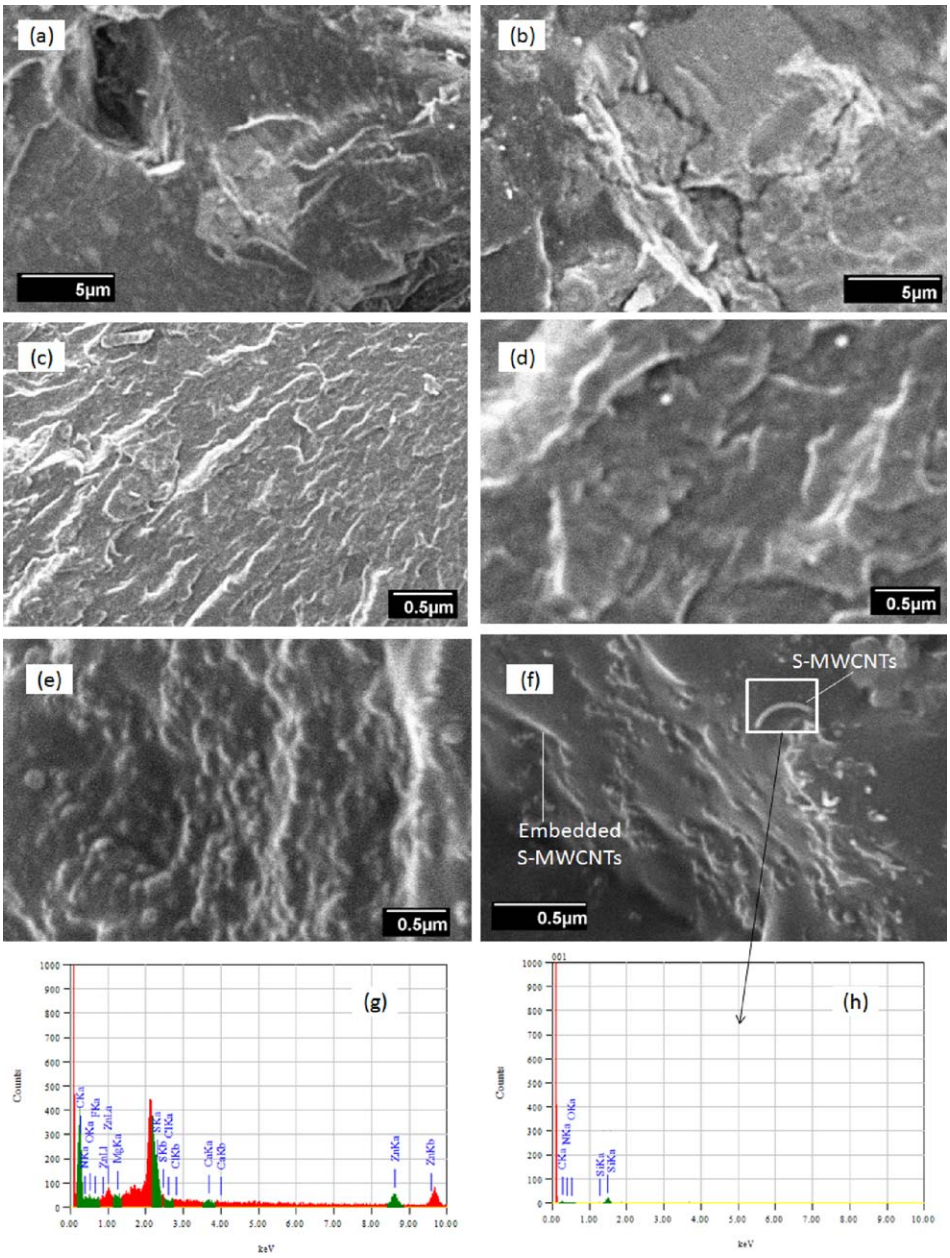

Figure 5. Distribution of S-MWCNTs within the polymer matrix at variant magnifications (a–f), compositional analysis of EPDM composite (g), and the embedded S-MWCNTs (h). [Color figure can be viewed in the online issue, which is available at wileyonlinelibrary.com.]

at 7. Centrifuge at 12,000 rpm for 30 min was used to recover the S-MWCNTs. The nanotubes sample was dried for overnight at 100°C to remove moisture from the specimen. The following results are obtained from FTIR, XRD, and SEM characterization to confirm of surface modification of S-MWCNTs.

Fabrication of S-MWCNT/EPDM Nanocomposites

S-MWCNTs was integrated into the rubber dispersion kneader at 110°C for 30 min to uniformly disperse and diffuse the nano fillers in the host polymer matrix with reinforcement (nanosilica), plasticizers (aromatic oil, wax), and activators (zinc oxide). The postmixing of the S-MWCNT/EPDM, blended rubber along with the addition of crosslinker (sulfur), and accelerators (MBTS and HBS) in the EPDM matrix was carried out on two roller mixing mill at 60°C and 40 rpm roller's speed for 20 min. Four precured rubber composite sheets with four diverse concentrations of S-MWCNTs were cultivated. The base formulation of S-MWCNT/EPDM nanocomposite (EC1) is presented in Table I. Five different concentrations of S-MWCNTs are included as 0.1 wt % (EC2), 0.3 wt % (EC3), 0.5% (EC4), and 1.0 wt % (EC5) in the basic composition 0 mass % (EC1). The composite specimens with dimensions 100 × 100 × 3 mm^3 for thermal transport analysis and tensile testing specimens according to ASTM D 412-98A, were cured on hot isostatic press at 130°C and 1500 psi for 30 min.

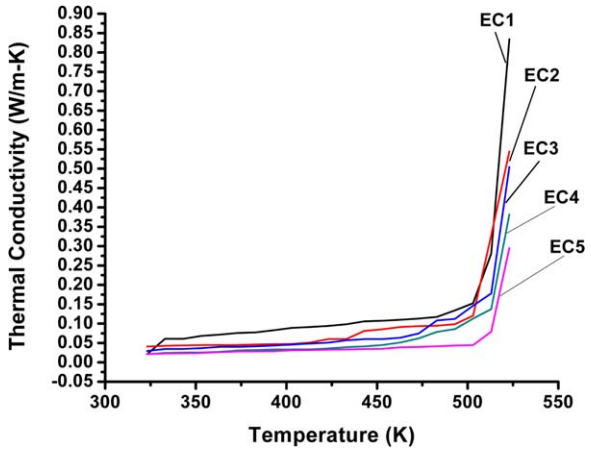

Figure 6. Thermal conductivity at different S-MWCNTs concentrations and temperatures. [Color figure can be viewed in the online issue, which is available at wileyonlinelibrary.com.]

RESULTS AND DISCUSSION

Confirmation of Silane Functionalization of MWCNTs

Figure 2(a) represents FTIR spectra of Ps-MWCNTs and S-MWCNTs. IR peak at 1463.32, 2900, and 1031.35 corresponds to silane moiety attachment as a result of the surface treatment. Crystalline nature of S-MWCNTs is also confirmed between 10° and 80° (2θ) XRD scan with a scanning step of 0.05°/min. Figure 2(b) shows the diffraction peaks at 26.71° and 44.91° corresponding to graphite structure derived from MWCNTs. Furthermore, the intensity of (002) and (100) peaks of S-MWCNTs are much closer to Ps-MWCNTs, provides the evidence for the fact that the treatment does not damage the graphene layer organization. TG/DTA was used to determine the thermal degradation behavior and heat absorbing capability of Ps/S-MWCNTs. Figure 2(c) represents the TGA and DTA traces of Ps/S-MWCNTs between 25 and 800°C under the oxygen environment. Thermographs clear that S-MWCNTs thermally

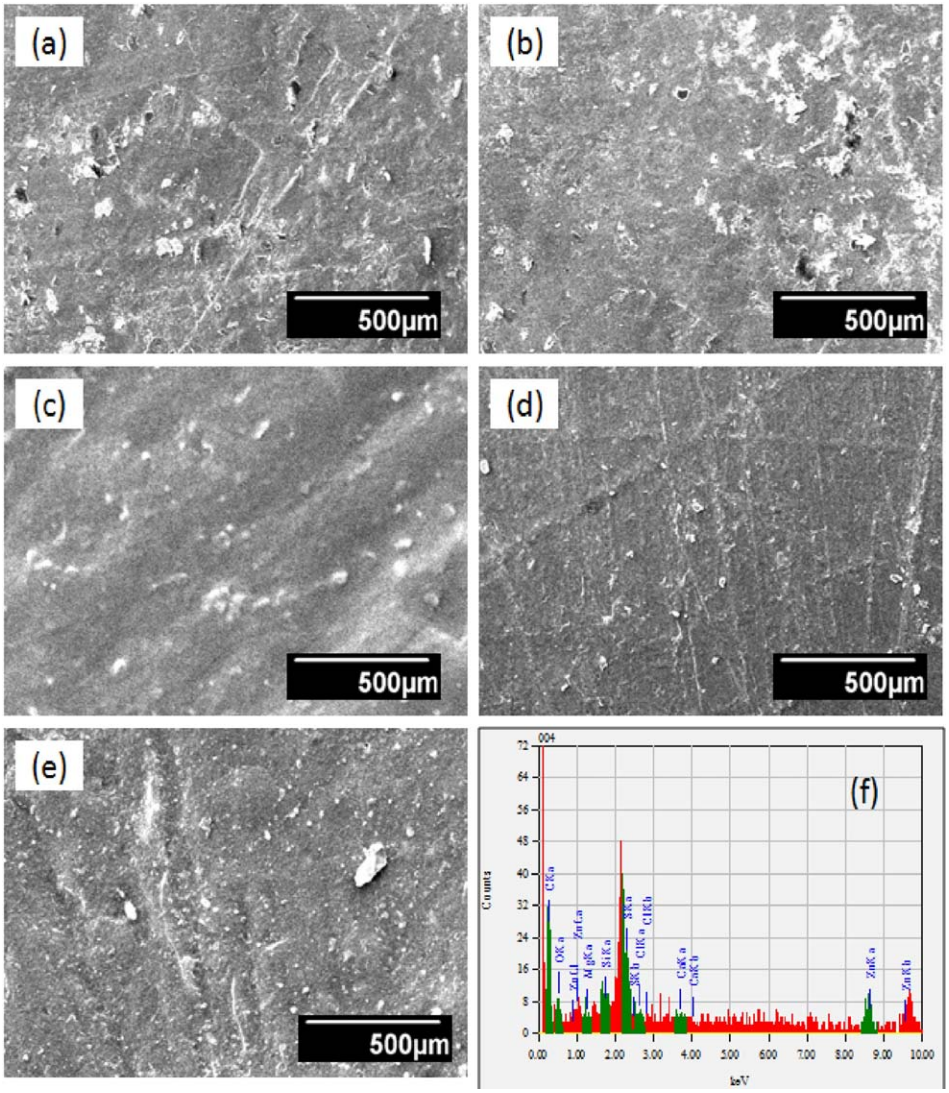

Figure 7. SEM micrographs of post-thermal transport tested nanocomposite specimens EC1 (a), EC2 (b), EC3 (c), EC4 (d), EC5 (e), and the compositional analysis of the1 wt % loaded S-MWCNTs in EPDM rubber (f). [Color figure can be viewed in the online issue, which is available at wileyonlinelibrary.com.]

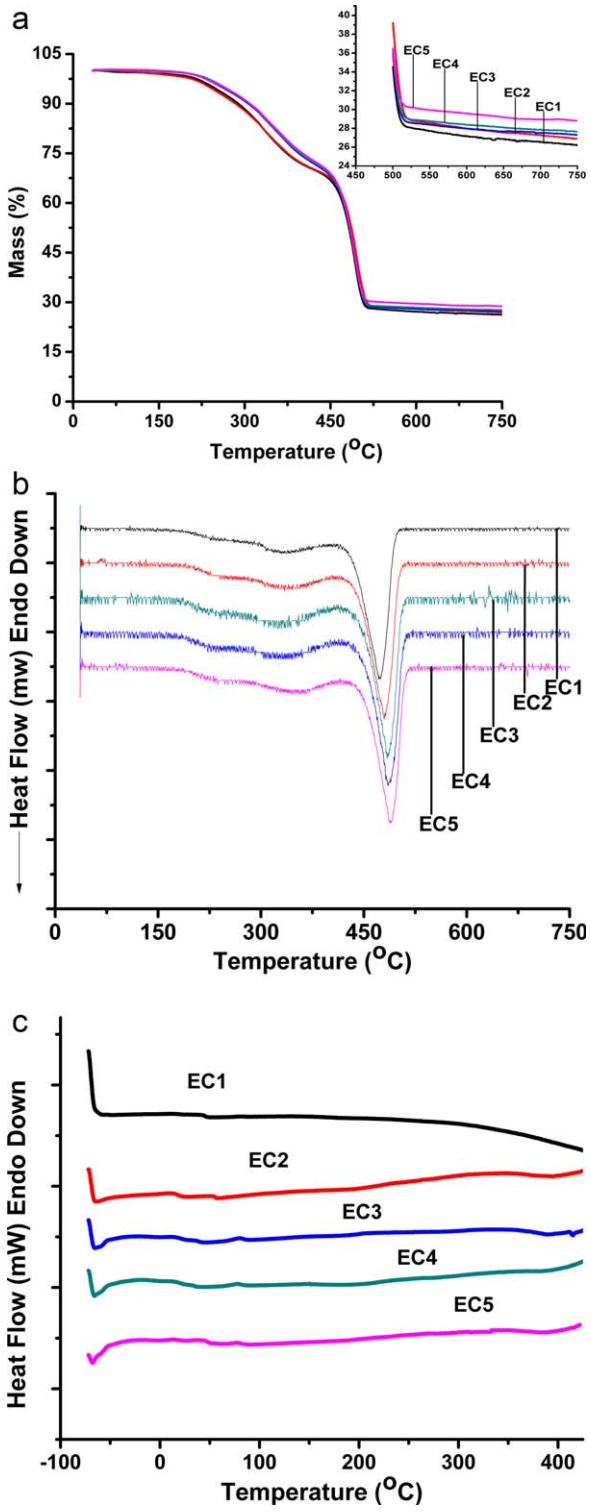

Figure 8. (a) Thermal decomposition analysis of S-MWCNT/EPDM nanocomposites. (b) Differential thermal analysis of S-MWCNT/EPDM specimens. (c) DSC contours of the fabricated S-MWCNT/EPDM composites. [Color figure can be viewed in the online issue, which is available at wileyonlinelibrary.com.]

degrade 13% in excess than Ps-MWCNTs counterpart due to silane debonding from S-MWCNTs surface in the form of water vapors NO_2 and CO_2 exhaust. In DTA curves, it is clear that S-MWCNTs absorb more heat than Ps-MWCNTs due to bond cleavage of covalently attached moieties on the surface of MWCNTs. SEM coupled with EDS was performed to investigate the morphology/compositional analysis of Ps-MWCNTs and S-MWCNTs. CNTs were coated with gold to make them more conductive for SEM analysis. The SEM comparative analysis of Ps-MWCNTs and S-MWCNTs morphology was carried out as shown in Figure 3(a,b) microscopic analysis confirms S-MWCNTs deagglamoration as a result of surface treatment of pristine nanotubes. Figure 3(c,d) depicted the compositional analysis (EDS) for both pristine/silane functionalized MWCNTs (Ps/S-MWCNTs) which clears the presence of elements other then carbon viz. Si, O, and N. These elements confirm the presence of silane moiety on the surface of nanotubes. EDS analysis endorsees FTIR spectra of Ps/S-MWCNTs.

Scanning electron microscopic analysis [Figure 4(a–d)] of the tensile fractured specimen (1 wt % pristine MWCNTs incorporated EPDM nanocomposite) at different magnifications and regions revealed the presence of agglomerated bundles of the incorporated nanotubes due to the presence of strong van der walls interaction among themselves.[18] Consequently, the doped nanotubes did not distributed uniformly within the host matrix and cause a stress concentrated region around the nanotubes cluster that may act as an impurity in the developed composite that may resulted composite failure when applied external load. The elemental analysis confirms the composition of pristine MWCNTS [Figure 4(e)]. Functionalization is therefore recommended before the incorporation of MWCNTs in the host matrices to develop covalent interaction/bonding among the nanotubes surface and host polymeric chains to maximize the reinforcing effects of the impregnated functionalized nanotubes on the dispersion, thermomechanical, and electrical properties of the developed composites as presented in the contemporary data.[19,20] So, the functionalizations and deagglamoration of nanotubes enhances the filler to polymer compatibility and dispersibility within the elastomeric matrix. Silane moiety makes correction with in polymeric chains to develop covalent interaction. This phenomenon leads to improve thermal stability as well as mechanical strength of the elastomeric system.

Even Dispersion of S-MWCNTs in EPDM Matrix

The dispersion of nanotubes in EPDM rubber matrix is analyzed by SEM micrographs at different magnifications, i.e., depicted in Figure 5(a–f). The compositional analysis of polymer nanocomposite [Figure 5(g)] elaborates the presence of the zinc, carbon, sulphur, oxygen, nitrogen, Mg etc that confirms the composite formulation scheme. Figure 5(h) demonstrates the EDS analysis of impregnated nanotubes within the elastomeric matrix. The obtained results show the presence of 100% confirming the nanotubes existence within the elastomeric nanocomposite.

Thermal Properties

Thermal conductivity of S-MWCNT/EPDM nanocomposite was measured in temperature range 323–532 K under steady state heat conditions and the accumulated data are presented in Figure 6. The thermal conductivity of the nanocomposite specimens reduces with increasing filler to matrix ratio. Bryning

Table II. Effect of Variant Concentrations of S-MWCNTs on the Glass Transition, Crystallization, and First/Second Melting Phase Temperatures of EPDM Nanocomposites

Sample ID	Glass transition temperature (T_g, °C)	Crystallization temperature (T_c, °C)	First melting temperature (T_{m1}, °C)	Second melting temperature (T_{m2}, °C)
EC1	−10.35 ± 0.10	4.25 ± 0.10	232.54 ± 0.10	384.47 ± 0.10
EC2	−12.47 ± 0.10	6.45 ± 0.10	240.32 ± 0.10	387.17 ± 0.10
EC3	−17.41 ± 0.10	7.45 ± 0.10	266.55 ± 0.10	388.52 ± 0.10
EC4	−19.23 ± 0.10	9.32 ± 0.10	271.94 ± 0.10	391.52 ± 0.10
EC5	−20.01 ± 0.10	11.82 ± 0.10	290.83 ± 0.10	395.26 ± 0.10

et al.[21] reported that the thermal conductivities of the surfactant-SWNT/epoxy composites are much lower (and the interfacial thermal resistances are higher) than that of the composites prepared without surfactant at the same loading. The maximum reduction is observed, i.e., 95% at 373 K for EC5 relative to base composite formulation, EC1. The 1 wt % S-MWCNTs incorporated rubber nanocomposite has 29% (at 373K) improved thermal impedance compared to the EC1 formulation due to the heat quenching through phonon entrapping by the incorporated nanotubes.[22,23] It is also attributed to uniform dispersion of S-MWCNTs within the host matrix. It may also attribute to heat absorption by silane moiety present on the surface of the nanotubes. Relatively low thermal conductivity of S-MWCNTs compared to the carbon black, also imparts an important role to minimize thermal transport through the fabricated composite specimens. Thermal conductivity of EPDM composites is reduced with increasing environment temperature due to the activation of processing aids evaporation, polymer pyrolysis, and endothermic phenomena within the polymer nanocomposite.[24–28]

Figure 7(a–e) represents the surface morphology of the composite specimens (EC1-EC5, respectively) with diverse S-MWCNTs concentrations after thermal transport testing. The presented figure shows that with increasing the S-MWCNTs loading in the rubber matrix, fabricated composite sustainability enhances in the analogs fashion. The incorporated S-MWCNTs have augmented thermal stability and diminished surfaced damage in heating environment due to their higher thermal endurance, surface area, and strong entanglement with the matrix polymeric chains. The uniform distribution and surface modification of the impregnated nanotubes also impart an important role to develop the S-MWCNTs network within the rubber matrix that enhances its thermal stability/resistance. The major elements C, S, Si, Zn, O, Mg, and Ca were found in the EDS analysis of EC5 due to presence of carbon black, S-MWCNTs, ZnO as activator, sulphur as a crosslinker, MgO and SiO_2 were the impurities in the incorporated fillers and processing aids, i.e., depicted in Figure 7(f).

Thermogravimetric analysis of the nanocomposites in temperature range 25–750°C is presented in Figure 8(a) shows a two-step thermal degradation. The primary thermal decomposition is observed in the temperature range 200–450°C due to the evaporation of aromatic oil, wax, and other processing ingredients. The secondary thermal oxidation is seen in the temperature range 450–520°C due to the EPDM pyrolysis. The introduction of S-MWCNT into the rubber matrix has enhanced the thermal stability of the fabricated nanocomposites due to high thermal endurance and nanoscale interaction of the nanotubes that restricts the thermal motion of molecular polymer chains in heating environment.[6,10] Thermal stability improvement up to 4% at 600°C was observed with the peak incorporation of S-MWCNTs into the host matrix.[29,30]

Figure 8(b) elucidates effective augmentation in heat absorbing capability with increasing the nanotubes loading in EPDM matrix. Chen *et al.*[31] concluded that thermal stability increasing with incorporation of MWCNTs. Heat quenching capability is also improved with increasing the nanotubes contents in the host matrix. The peak melting temperature is moved towards the higher temperature with increasing the concentration of S-MWCNTs in the polymer matrix which is evidence of thermal stability enhancement of the nanocomposites as proved from TGA thermograms.

Figure 8(c) elucidates the differential scanning calorimetric study to understand the influence of S-MWCNTs on the glass transition (T_g), crystallization (T_c), and onset melting (T_{m1}), and peak melting temperature (T_{m2}) temperatures of the composite specimens. The acquired data of these phase changing temperatures are presented in Table II from the DSC contours. T_g of the composite specimens has been reduced with the

Table III. Effect of Variant Concentrations of S-MWCNTs on the Specific Enthalpies (T_g, T_c, T_{m1}, and T_{m2}) of EPDM Nanocomposites

Sample ID	EC1	EC2	EC3	EC4	EC5
Specific enthalpy of glass transition (J/g)	3.21 ± 0.01	1.95 ± 0.01	1.82 ± 0.01	1.42 ± 0.01	1.19 ± 0.01
Specific enthalpy of crystallization (J/g)	0.12 ± 0.01	0.13 ± 0.01	0.14 ± 0.01	0.16 ± 0.01	1.26 ± 0.01
Specific enthalpy of onset melting phase (J/g)	5.69 ± 0.01	16.99 ± 0.01	17.64 ± 0.01	22.78 ± 0.01	35.57 ± 0.01
Specific enthalpy of peak melting phase (J/g)	15.70 ± 0.01	16.46 ± 0.01	33.67 ± 0.01	46.39 ± 0.01	54.29 ± 0.01

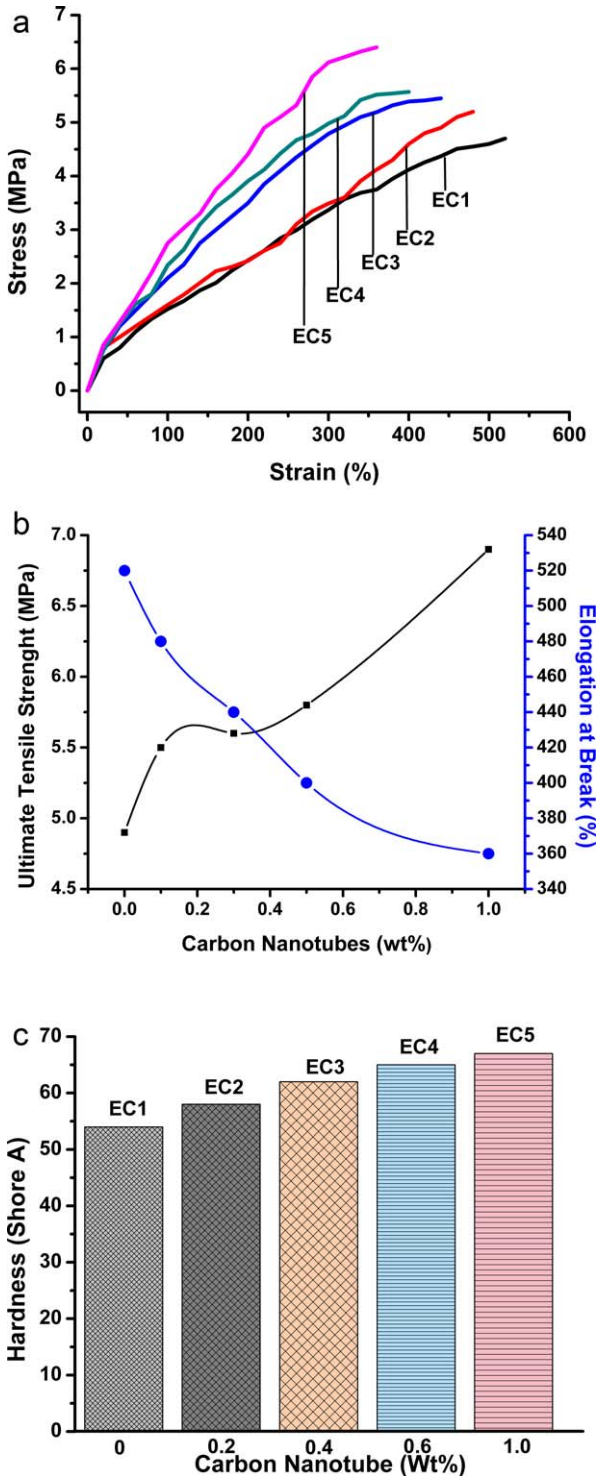

Figure 9. (a) Effect of different doping concentrations of S-MWCNT on stress–strain performance of EPDM nanocomposites. (b) Effect of different doping concentrations of S-MWCNT on ultimate tensile strength and percent elongation at break of EPDM nanocomposites. (c) Effect of different doping concentrations of S-MWCNT on shore A hardness of EPDM nanocomposites. [Color figure can be viewed in the online issue, which is available at wileyonlinelibrary.com.]

incorporation of nanotubes in the polymer matrix. The reverse response is observed for T_c. It attributed to S-MWCNT network in the polymer matrix that constraint the phase changes by interacting with the polymeric chains at nanoscale and broadens rubbery phase of the fabricated polymer nanocomposites. Consequently, EC5 nanocomposite can be operated in more negative temperature compared to other ones up to −20°C . T_{m1} and T_{m2} respectively, are enhanced up to 58.28 and 11.21°C, respectively because nanotubes have offered much resistance to the matrix molecular chain mobility by entrapping phonons within the filler's network. Another major reason of the melting temperature enhancement is the higher thermal stability of incorporated S-MWCNTs compared to carbon black.[32,33]

Glass transition and crystallization are exothermic phenomena, but melting of the polymer composite is an endothermic phenomenon which means that the nanotubes impregnation in the carbon-filled EPDM composite enhances the endothermic behavior of the composite specimens. Specific enthalpies of the nanocomposite specimens are depicted in Table III. It is observed that specific enthalpy of glass transition phase is reduced with increasing nanotubes to matrix ratio. The specific enthalpies of crystallization, onset, and peak melting phases are elevated due to enhancement in endothermic nature and thermal endurance of the nanocomposite with increasing the doping concentration of nanotubes in the rubber matrix. This phenomenon is also endorsed by the DTA thermograms.[1]

Mechanical Properties

Stress–strain contours of the nanocomposites are displayed in Figure 9(a) that shows an augmentation in tensile strength while elongation at break suffers with the progressive addition of carbon nanotubes in the EPDM rubber matrix. Bokobza *et al.* measured the tensile strength 5.5 MPa. Perez *et al.*[13] prepared MWCNT/NBR nanocomposites with improved tensile strength (UTS is 36% higher). Girun *et al.*[34] reported UTS around 1.25 MPa. Figure 9(b) shows that 1 wt % incorporation of S-MWCNTs in the rubber matrix elevates the tensile strength and elastic modulus up to 41 and 111%, respectively. It is attributed to even dispersion of nanotubes in the polymer matrix, strong MWCNT–polymer interaction, and superior mechanical strength of the carbon nanotubes. A progress in shore A hardness of the composite specimens is observed in Figure 9(c) with increasing filler contents in the rubber matrix. The addition of S-MWCNTs in the host polymer matrix augments the rubber hardness due to strong interaction of nanotubes to polymeric chains of the EPDM. Another reason to enhance elastomeric hardness is reduction of chain mobility with increasing S-MWCNTs concentration in the host matrix.[26,35–37]

CONCLUSION

The progressive incorporation of silane functionalized carbon nanotubes into the polymer matrix has remarkably enhanced the thermal and mechanical performance of the nanocomposites. Thermal transport study reveals that the incorporation of S-MWCNTs into the EPDM matrix has effectively enhanced the thermal resistance of the fabricated composite specimens up to 95%. Thermal stability and endothermic capability of the fabricated composites are improved remarkably with the nanotubes introduction into the

rubber matrix. DSC study illustrates the S-MWCNTs incorporation into the base composite formulation has successfully increased the melting temperature and reduced the glass transition temperature of the developed composites. Ultimate tensile strength and shore A rubber hardness and elongation at break of the rubber nanocomposites have been improved with increasing filler to matrix ratio due to the even dispersion, durable filler to matrix bonding, and excellent mechanical strength of S-MWCNTS.

ACKNOWLEDGMENTS

The authors would like to greatly acknowledge Start Up Research Grant program (SRGP) from Higher Education Commission (HEC) of Pakistan (No.: 21-433 SRGP/R&D/HEC/2014) for providing sufficient funds to execute this research, School of Chemical and Materials Engineering (SCME), National University of Sciences and Technology (NUST), and Longman Mills, Lahore to facilitate us with the best of their rubber nanocomposite fabrication and testing expertise and facilities.

REFERENCES

1. Sagar, S.; Iqbal, N.; Maqsood, A.; Shahid, M.; Shah, N. A.; Jamil, T.; Bassyouni, M. I. *J. Compos. Mater.* **2014**, 0021998314528733.
2. Adohi, B. J. P.; Mdarhri, A.; Prunier, C.; Haidar, B.; Brosseau, C. *J. Appl. Phys.* **2010**, *108*, 074108.
3. Spitalsky, Z.; Tasis, D.; Papagelis, K.; Galiotis, C. *Prog. Polym. Sci.* **2010**, *35*, 357.
4. Su, Z.; Li, J.; Li, Q.; Ni, T.; Wei, G. *Carbon* **2012**, *50*, 5605.
5. Wang, H.; Li, J.; Zhang, X.; Ouyang, Z.; Li, Q.; Su, Z.; Wei, G. *RSC Adv.* **2013**, *3*, 9304.
6. Planeix, J.; Coustel, N.; Coq, B.; Brotons, V.; Kumbhar, P.; Dutartre, R.; Geneste, P.; Bernier, P.; Ajayan, P. *J. Am. Chem. Soc.* **1994**, *116*, 7935.
7. Xie, X. L.; Mai, Y. W.; Zhou, X. P. *Mater. Sci. Eng. R* **2005**, *49*, 89.
8. Bal, S. B. *Mater. Sci.* **2010**, *33*, 27.
9. Zhang, P.; Zhao, X.; Zhang, X.; Lai, Y.; Wang, X.; Li, J.; Wei, G.; Su, Z. *ACS Appl. Mater. Interfaces* **2014**, *6*, 7563.
10. Sun, Y. P.; Fu, K.; Lin, Y.; Huang, W. *Acc. Chem. Res.* **2002**, *35*, 1096.
11. Dyke, C. A.; Tour, J. M. *Chem. A: Eur. J.* **2004**, *10*, 812.
12. Saito, R.; Dresselhaus, G.; Dresselhaus, M. S. Physical Properties of Carbon Nanotubes; World Scientific: USA, **1998**.
13. Perez, L. D.; Zuluaga, M. A.; Kyu, T.; Mark, J. E.; Lopez, B. L. *Polym. Eng. Sci.* **2009**, *49*, 866.
14. Malas, A.; Das, C. K. *J. Mater. Sci.* **2012**, *47*, 2016.
15. Singh, S.; Guchhait, P.; Bandyopadhyay, G.; Chaki, T. *Compos. A: Appl. Sci.* **2012**.
16. Zeynali, M. E.; Yousefi, A. A.; Soltani, I. *Polym. Plast. Technol. Eng.* **2009**, *48*, 42.
17. Rajeev, R.; De, S.; Bhowmick, A. K.; John, B. *Polym. Degrad. Stab.* **2003**, *79*, 449.
18. Atieh, M. A. *Fuller. Nanotubes Carbon Nanostruct.* **2011**, *19*, 617.
19. Ganguli, S.; Aglan, H.; Dennig, P.; Irvin, G. *J. Reinfor. Plast. Compos.* **2006**, *25*, 175.
20. Thomas, P. S.; Abdullateef, A. A.; Al-Harthi, M. A.; Basfar, A. A.; Bandyopadhyay, S.; Atieh, M. A.; De, S. K. *J. Appl. Polym. Sci.* **2011**, *124*, 2370.
21. Bryning, M. B.; Islam, M. F.; Kikkawa, J. M.; Yodh, A. G. *Adv. Mater.* **2005**, *17*, 1186.
22. Aliev, A. E.; Lima, M. H.; Silverman, E. M.; Baughman, R. H. *Nanotechnology* **2010**, *21*, 035709.
23. Pham, D. C. *Int. J. Heat Mass Tranf.* **2008**, *51*, 3355.
24. Han, Z.; Fina, A. *Prog. Polym. Sci.* **2011**, *36*, 914.
25. Sagar, S.; Iqbal, N.; Maqsood, A.; Javaid, U. *J. Therm. Anal. Calorim.* **2013**, *114*, 161.
26. Ali Raza, M.; Westwood, A.; Stirling, C.; Brydson, R.; Hondow, N. *J. Appl. Polym. Sci.* **2012**, *126*, 641.
27. Masarapu, C.; Henry, L.; Wei, B. *Nanotechnology* **2005**, *16*, 1490.
28. Agari, Y.; Uno, T. *J. Appl. Polym. Sci.* **2003**, *30*, 2225.
29. Zhang, C.; Pal, K.; Byeon, J. U.; Han, S. M.; Kim, J. K. *J. Appl. Polym. Sci.* **2011**, *119*, 2737.
30. Iqbal, N.; Sagar, S.; Khan, M. B.; Rafique, H. M. *Polym. Eng. Sci.* **2013**, *54*, 255.
31. Chen, S.; Yu, H.; Ren, W.; Zhang, Y. *Thermochim. Acta* **2009**, *491*, 103.
32. Sagar, S.; Iqbal, N.; Maqsood, A. *J. Reinforced Plast. Compos.* **2013**, *32*, 1052.
33. Sagar, S.; Iqbal, N.; Maqsood, A. *J. Phys. Confer. Ser.* **2013**, 012024.
34. Girun, N.; Ahmadun, F. R.; Rashid, S. A.; Atieh, M. A. *Fuller. Nanotubes Carbon Nanostruct.* **2007**, *15*, 207.
35. Iqbal, N.; Khan, M. B.; Sagar, S.; Maqsood, A. *J. Appl. Polym. Sci.* **2013**, *128*, 2439.
36. Iqbal, N.; Sagar, S.; Khan, M. B.; Bassyouni, M. I.; Khan, Z. M. *J. Appl. Polym. Sci.* **2013**, *130*, 4392.
37. Sarkhel, G.; Choudhury, A. *J. Appl. Polym. Sci.* **2008**, *108*, 3442.